Nanoscale

Accepted Manuscript

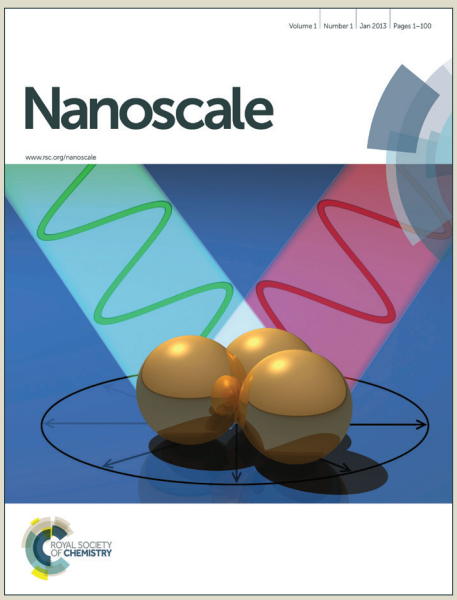

ROYAL SOCIETY OF CHEMISTRY

www.rsc.org/nanoscale

Dominant Luminescence is not Due to Quantum Confinement in Molecular-Sized Silicon Carbide Nanocrystals

David Beke[*†‡], *Zsolt Szekrényes*[†], *Zsolt Czigány*[§], *Katalin Kamarás*[†], *and Ádám Gali*[†#*]

[†]Institute for Solid State Physics and Optics, Wigner Research Centre for Physics, Hungarian Academy of Sciences, PO. Box 49, H-1525 Budapest, Hungary

[‡]Faculty of Chemical Technology and Biotechnology, Budapest University of Technology and Economics, Műegyetem rkp. 3., H-1111 Budapest, Hungary

[§]Institute for Technical Physics and Materials Science, Centre for Energy Research, Hungarian Academy of Sciences, Konkoly-Thege M. út 29-33., H-1121 Budapest, Hungary

[#]Department of Atomic Physics, Budapest University of Technology and Economics, Budafoki út 8, H-1111 Budapest, Hungary

ABSTRACT Molecular-sized colloid silicon carbide (SiC) nanoparticles are very promising candidates to realize bioinert non-perturbative fluorescent nanoparticles for *in vivo* bioimaging. Furthermore, SiC nanoparticles with engineered vacancy-related emission centres may realize magneto-optical probes operating at nanoscale resolution. Understanding the nature of

molecular-sized SiC nanoparticle emission is essential for further applications. Here we report an efficient and simple method to produce a relatively narrow size distribution of water soluble molecular-sized SiC nanoparticles. The tight control of their size distribution makes possible to demonstrate a switching mechanism in the luminescence correlated with particle size. We show that molecular-sized SiC nanoparticles of 1-3 nm show a relatively strong and broad surface related luminescence whilst larger ones exhibit relatively weak band edge and structural defect luminescence with no evidence of quantum confinement effect.

Table of Contents Figure

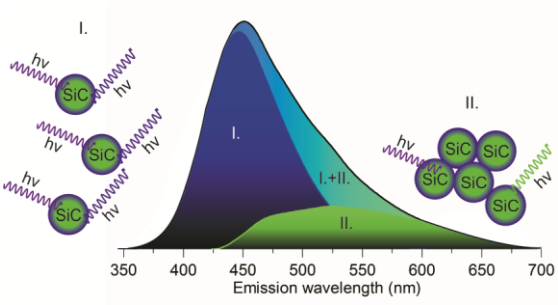

Successful size separation of SiC NCs demonstrates the coexistence of surface and band-edge related luminescence of these nanoparticles.

KEYWORDS:

silicon carbide,

quantum confinement,

bioimaging,

colloid quantum dots,

luminescence

Silicon carbide is a wide bandgap indirect semiconductor[1] with a variety of applications such as high power electronics due to the high breakdown field, high thermal conductivity, and existence of surface oxide[2]. Because of the chemical resistivity and high intrinsic temperature SiC is ideal for applications in harsh environments[3]. It also exhibits great application potential in ultraviolet (UV) photodiodes[4], spintronics[5,6] and quantum information processing[7,8,9]. SiC can crystallize in several forms called polytypes. These polytypes are identical in two dimensions (hexagonal basal plane) and differ in the Si-C bilayer sequences in the third dimension (c-axis perpendicular to the basal plane)[10]. As an indirect-bandgap semiconductor, bulk SiC has weak luminescence, however, porous SiC[11], small nanocrystals[12] and nanowires[13] show bright photoluminescence (PL). SiC nanocrystals (NCs) are proven to be favorable biological labels[14] due to their good biocompatibility,[15] hemocompatibility[16] and excellent solubility in polar solvents[17]. Moreover, they contain many surface groups that are suitable for further chemical modifications and conjugation for targeted biomolecules[18]. Even though the applicability of SiC NCs in biological environment[19,20] and therapy[21] was demonstrated, understanding the physics behind the luminescence is still in the centre of intense research. In porous SiC bright luminescence was reported, similar to that in porous Si, but the origin of this luminescence is still unclear. The luminescence of porous SiC is often associated with the quantum confinement effect,[22] however, the relatively large crystallite size and the polytype independent luminescence implied that the luminescence was related to surface defects[23]. Experimental results[24,25] and theoretical calculations showed that the luminescence of SiC NCs is strongly influenced by the surface groups[26]. Indeed SiC NCs solution containing 2-nm nanoparticles shows luminescence with emission at 450 nm (2.75 eV), nearly independent of excitation wavelength, while calculation showed that hydrogen terminated NCs with this size should emit in the deep UV[27,28].

Wu and coworkers stated experimental evidence of quantum confinement in SiC NCs[29] based on the excitation dependent luminescence properties of such NCs solution. This dependence is a necessary but not sufficient condition to unambiguously prove the quantum confinement effect. There are several reports about excitation dependent luminescence properties of carbon dots[30,31] and graphene oxide solutions[32] where this property is explained by different surface groups and the distribution of these groups[33]. Guo *et al*. reported that SiC NCs prepared in ethanol solution possessed low excitation dependent emission in the case of fresh samples but aged samples showed strong excitation dependence[34]. Their size measurements suggested that SiC NCs aggregated quickly in ethanol solution and they associated the changes in the luminescence properties with the change in size distribution of SiC NCs[34]. These contradicting results shed doubt on the simple quantum confinement model and the varying conclusions might come from the different size distribution of the colloid SiC particles.

In this paper we demonstrate an effective size separation method which allows us to prepare a SiC NCs solution containing only 1-4 nm particles. This is an important step toward biomedical and *in vivo* applications where the hydrodynamic size of the nanocrystals should be less than 5.5 nm needed for clearance[35,36]. With the separation of small individual SiC NCs from larger or aggregated NCs we show that SiC NCs larger than 4 nm have different PL properties than those of molecular-sized nanoparticles. We demonstrate that the obtained excitation dependence of SiC NCs solution in previous reports is a convolution of two different emission centres with different PL and different photoluminescence excitation (PLE) properties because of the coexistence of molecular-sized 1-4 nm nanoparticles with surface related luminescence and larger nanoparticles or aggregates with band edge (BE) or near band edge (NBE) luminescence.

The recorded PL spectra of as-prepared SiC NCs are shown in **figure 1**. As can be seen the peak maximum at ~450 nm shifts only 8 nm upon changing the excitation wavelength between 310-370 nm (marked with a vertical dashed line) but shows a severe reduction in the measured intensity upon excitation with wavelengths longer than 320 nm. We observe another more intense red shift upon excitation with wavelengths of 370-450 nm (marked by the slant dashed line). This shift was previously associated with the quantum confinement effect[29]. We will demonstrate that this shift is due to the convolution of two different emission centres.

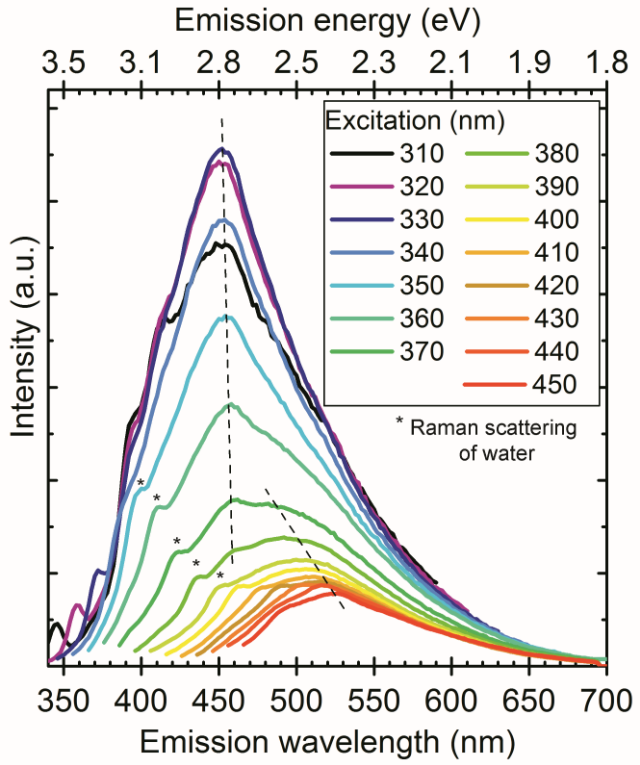

Figure 1. Photoluminescence spectra of SiC NCs in water at different excitation wavelengths. We attribute this complex spectrum to two types of emission centres represented by dashed lines. An emission centre at ~450 nm (vertical dashed line) shows a negligible red shift with

increasing excitation wavelengthwavelength whereas another emission centre at the low-frequency shoulder shows a clear red shift by varying the excitation wavelength between 370-450 nm represented by the slant dashed line. The Raman signal of water is also marked in the spectrum by star symbols.

A sample with broad size distribution was centrifuged through a 30 kDa macrosep filter. The remaining solution (sample II) was washed 10 times to remove most of the small particles. It should be noted that the feed was concentrated from 10 ml to 1.5 ml during filtration but not dried. As shown in **figure 2a,** that filtrate (sample I) exhibits a similar peak maximum as the as-prepared sample but the long-wavelength shoulder is missing and there is almost no sign of changing the emission with excitation wavelength.

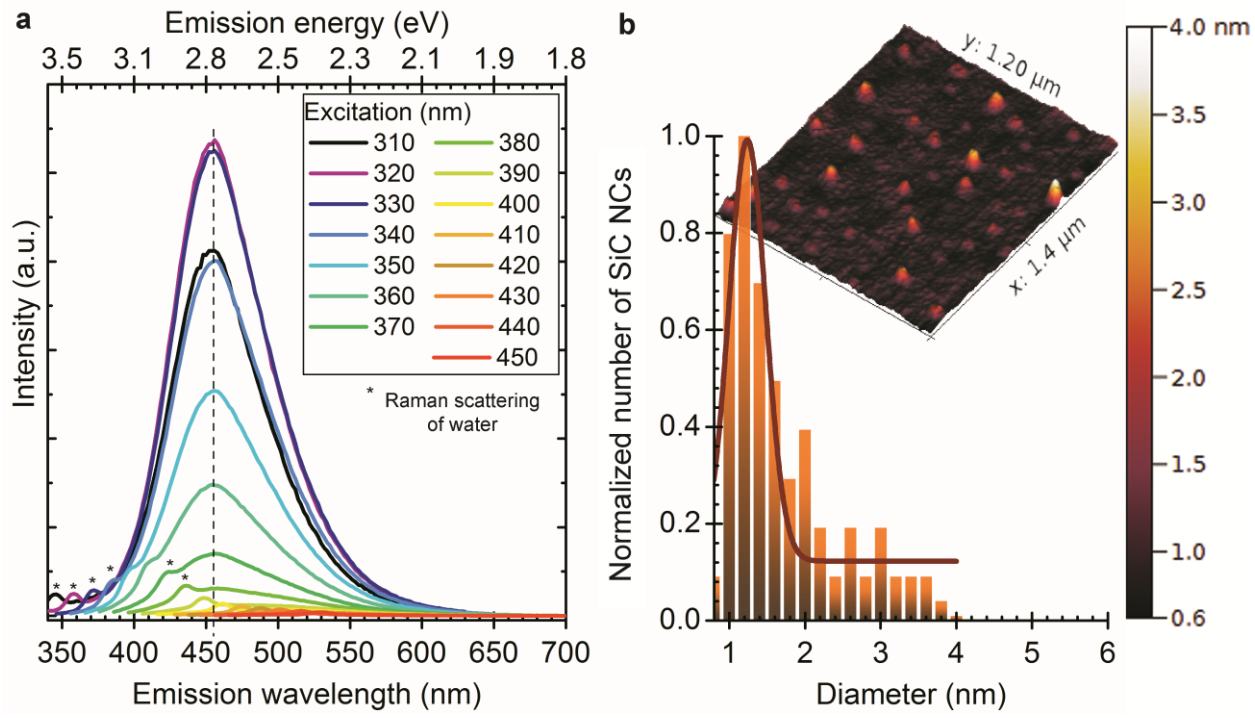

Figure 2. a shows the PL spectra of sample I (filtrate) at different excitation wavelengths after SiC NCs were filtered through a 30 kDa centrifuge filter. After filtration the red shoulder does not occur in the PL spectra (c.f, **figure 1**). **b** shows the AFM image and size distribution of sample I. The average size is about 1.5 nm and most of the particles are smaller than 4 nm.

Figure 3a-c and **3d** show the size and atomic structure of sample II observed by high transmission resolution spectroscopy (HRTEM) and atomic force microscopy (AFM), respectively, whereas **Figure 3e** plots the corresponding PL spectra**.** The PL spectra of sample II show excitation independent emission with peak maximum at 530 nm (2.39 eV). The shape and intensity of the luminescence band are very different from those of sample I.

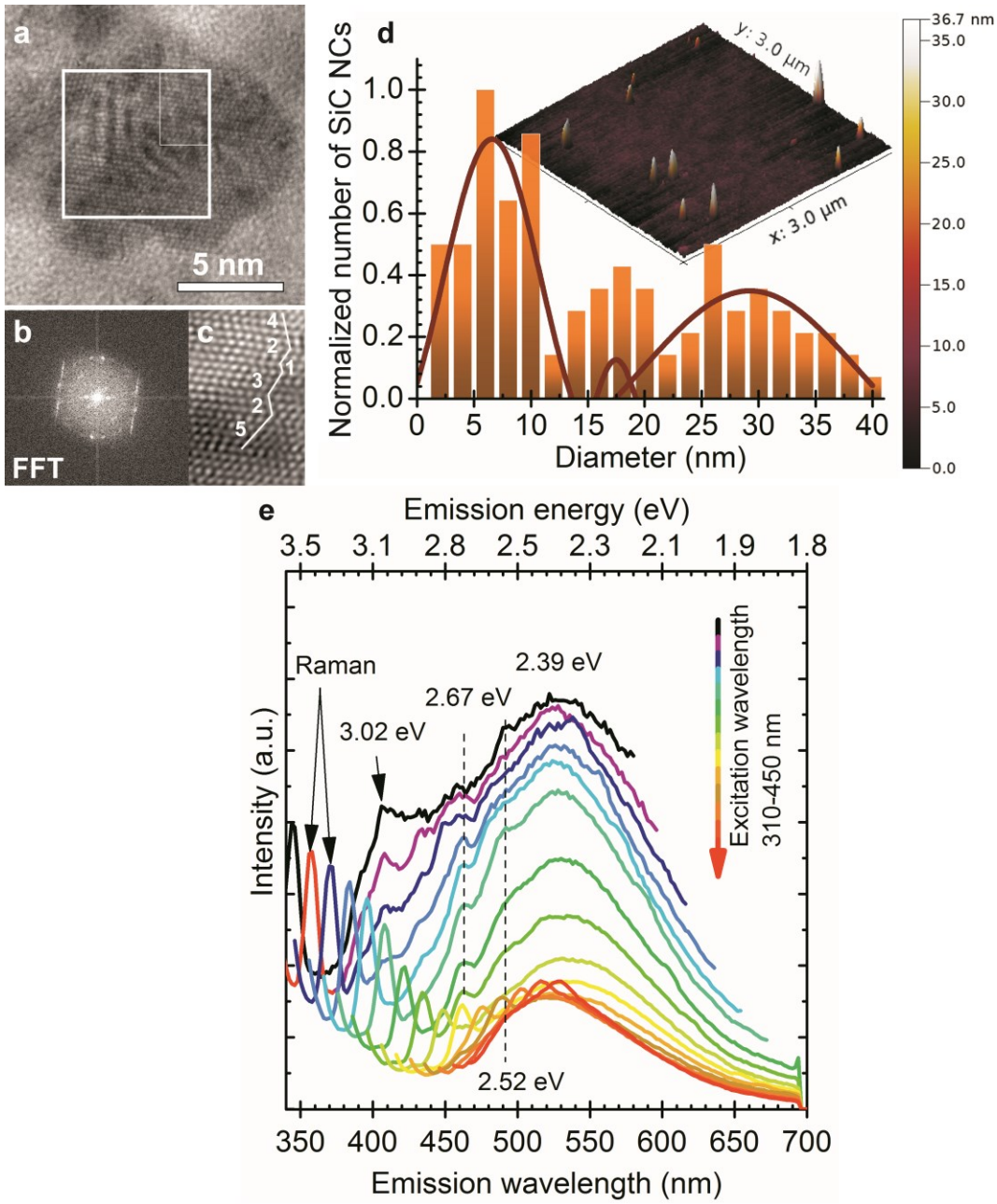

Figure 3. a HRTEM image of a ~10nm SiC nanoparticle. **b** Fast Fourier transform (FFT) of the area marked with square in panel **a**. **c** Fourier filtered HRTEM image of the area marked with a rectangle in the upper right corner of the square in panel **a**. An irregular stacking sequence of 5-2-3-1-2-4 is indicated in the figure. See text for more explanation. **d** shows AFM image and

the size distribution of sample II. Sample II contains particles with size between 2 and 40 nm. 3 Gauss functions can be fit to the size distribution with maxima at 6.5 nm, 17.5 nm and 29.0 nm. **e** PL spectra of sample II (filtrand) at different excitation wavelengths after SiC NCs were filtered through a 30 kDa centrifuge filter. The broad peak at 530 nm (2.39 eV) is the BE luminescence of SiC while peaks at 408 nm (3.02 eV), 464 nm (2.67 eV) and 492 nm (2.52 eV) are associated with the BE of 6H polytype inclusions (sequence of 3 in **c**) and their stacking faults (sequences other than 3 in **c**). The Raman peaks of the absorbed water are also indicated ('Raman') that have comparable intensity to that of the detected PL of SiC particles.

Despite the wide size distribution no shift occurs in the emission maximum upon changing the excitation wavelength. The 530 nm (2.39 eV) PL signal is in good agreement with the band gap of 3C-SiC (2.35 eV). The Bohr radius of 3C-SiC is about 2.7 nm and calculations implied that 4-nm 3C-SiC NCs have an almost bulk like absorption band [28]. Based on these arguments we attribute the 530-nm peak to the BE luminescence of larger particles. While SiC has an indirect band gap, consequently weak luminescence at room temperature, exciton recombination can be enhanced by the relaxation of selection rules due to the relatively small size of the particles and dielectric confinement. Several additional peaks appear in the PL spectra of sample II at about 408 nm (3.02 eV), 460 nm (2.67 eV) and 492 nm (2.52 eV). The first peak may correlate with the BE luminescence of 6H polytype inclusions[37] whilst the other two may originate from their stacking faults[38]. 6H inclusion in 3C-SiC may be considered as an "ordered" sequence of stacking faults that can be described as 3-3 zig-zag lines consisting of 6 Si-C bilayers along the c-axis (see Supplementary Information). Stacking faults within the 6H inclusions embedded in 3C-SiC result in irregular stacking sequences. We show the evidence of such irregular stacking

sequences in a larger SiC nanoparticle observed by HRTEM in **figure 3(a-c)**. Even though the purchased SiC is cubic 3C powder confirmed by X-ray diffraction measurements before and after etching it (not shown), polytype inclusions are common defects in SiC and may appear at low concentrations in the 3C-SiC powder. Since the applied etching method works mainly on the cubic 3C-SiC[39], the hexagonal polytypes remain mostly intact. Therefore, selective etching of 3C-SiC enhances the concentration of polytype inclusions in our system. While we believe this is the main reason of the detected polytype dispersion, it should be noted that phase transformation was claimed during preparation of SiC NCs by laser ablation[40] and also by an etching process similar to ours[34]. 6H inclusions in 3C-SiC enhance the luminescence of 3C-SiC[41] which further explains the detectable BE luminescence of 3C-SiC at room temperature. **Figure 4** shows the photoluminescence excitation (PLE) spectra of sample I and sample II. Sample I has maximum emission efficiency at 320 nm excitation while the PLE spectrum of sample II corresponds to the PLE of bulk 3C-SiC[42]. These observations further strengthen our conclusion that the properties of large particles are close to those of bulk 3C-SiC.

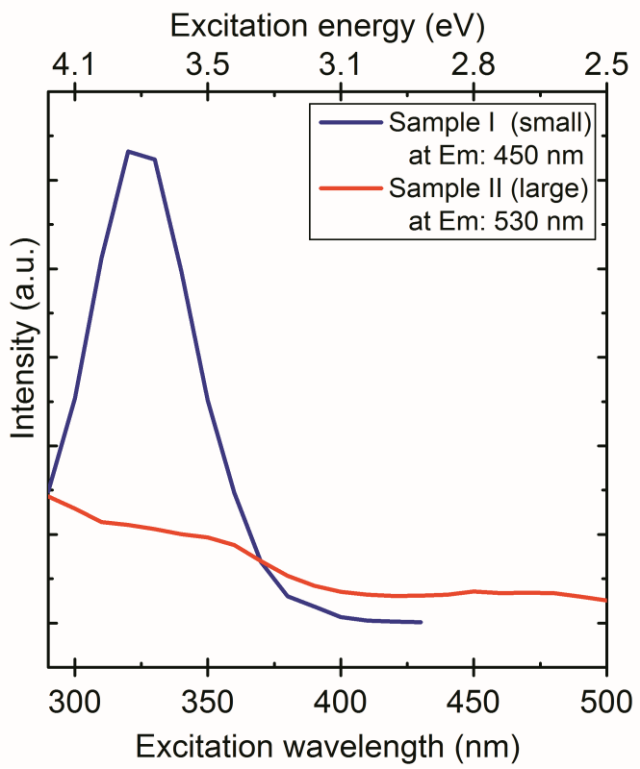

Figure 4. PLE spectra of SiC NCs with different size distribution where the emission wavelength ("at Em:") is indicated. Sample I contains 1-4 nm particles, sample II contains particles larger than 5 nm. The different lineshapes confirm that different absorption and emission mechanisms take place in these two systems.

Large particles may either form because of the repeated etching of SiC powder reducing the size of the starting materials or may come from the aggregation of smaller particles. To unravel the role of either of these mechanisms in the change of the luminescence band we dried a droplet of sample I on Si surface consisting of only molecular-sized nanoparticles and measured the PL during drying. **Figure 5** shows how the PL changed during water evaporation. First, SiC NCs are surrounded with strongly adsorbed water molecules[24], thus the PL of this sample is almost

identical to the PL of SiC NCs in solution. As we successively remove the hydration shell around the SiC nanoparticles, the emission maximum shifts to lower wavelengths typical of the PL signal of sample II. We conclude from the change in the PL bands that water evaporation is a two-step process: first the disappearance of the excess water, leaving the hydrated nanoparticles intact, followed by the disruption of the hydration shells and the subsequent forming of aggregates which leads to the PL bands characteristic of sample II. This result indicates that sample II may contain aggregates.

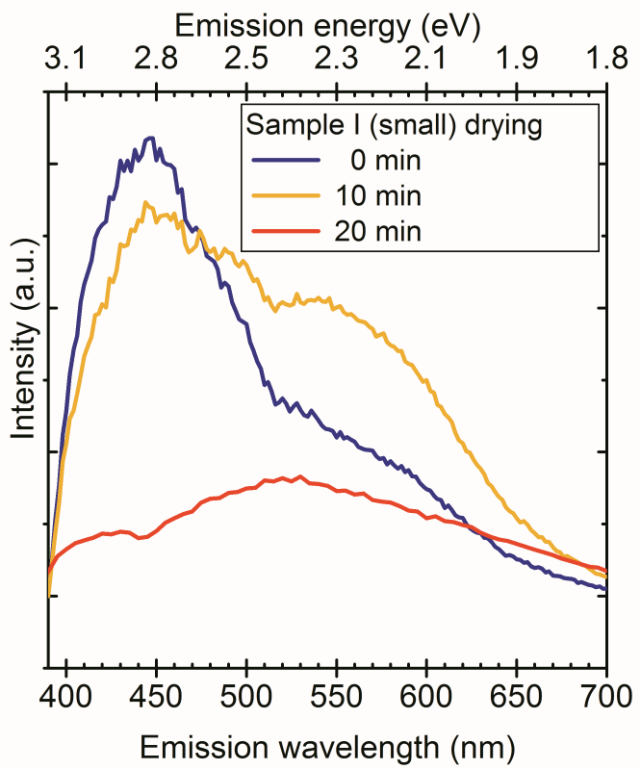

Figure 5. PL spectra of SiC NCs solution containing small particles during drying on Si surface. The emission is changing due to water evaporation and aggregation. The measurement was

carried out by heating the sample on a 100 °C hot plate at and placing it into the spectrometer at 5-minute intervals.

Aggregated or closely packed NCs usually have different optical properties from those of the individual particles[43,44]. It should be noted that even though surfactants are not used to stabilize our SiC NCs because of the high colloid stability of the particles, recrystallization or Ostwald ripening effect is not probable because of the high stability of the Si-C bond. The wavefunctions in two closely lying SiC NCs may overlap building up crystalline bands[43,45] that can lead to bulk-like optical properties. This effect is known in similar nanoparticle systems[43–45].

We did not find any sign of size dependent optical properties in the 3C-SiC colloid system, however, the size distribution was relatively broad in both parts of the separated samples. SiC NCs made by electroless wet chemical etching contain a large number of oxidized surface groups because of the applied strong acids. We conclude that SiC NCs could be rather described as $Si_xC_yO_z(H)$ systems. In the case of molecular-sized SiC NCs surface related luminescence is dominant[34,46]. The surface related luminescence originates from localized states that have weak NC size dependency[47]. However, various oxygen-containing surface groups may contribute to the PL spectrum depending on the surface environment possessing considerable Stokes shifts[24,26,27] that result in a relatively broad PL signal at room temperature**.** As the particles become larger, the surface to volume ratio becomes small and the oxygen content becomes negligible. Our results confirm the conclusion of theoretical calculations stating [27,46] that the core recombination becomes dominant for nanoparticles with size of 4 nm and above while surface related luminescence dominates in smaller SiC nanoparticles.

In conclusion, we demonstrated an effective separation of molecular-sized bioinert SiC nanoparticles from larger aggregates in colloid SiC NCs solution. These two fractions possess significantly different PL signals. PL is proven to be a very simple and efficient tool to verify the presence of larger aggregates in the colloid samples using a PL peak at around 530 nm. Our results show that the molecular-sized SiC NCs indeed exhibit surface group-related broad luminescence between 400 and 600 nm with a maximum at 450 nm. This broad luminescence may play an important role in the context of magneto-optical color centres in nanocrystalline SiC[48,47]. It has been proposed that molecular-sized SiC NCs embedding paramagnetic color centres may be ultimate fluorescent biomarkers that might be used even for quantum metrology going beyond the traditional dyes[14]. We demonstrated here that molecular-sized SiC NCs themselves possess complex emission properties. We note that the fluorescence of color centres introduced in these SiC NCs might be compromised by the surface groups responsible for the emission of SiC NCs which is a subject of studies in the near future.

Experimental Section

3C-SiC powder with particle sizes of about 1-10 μm (US Research Nanomaterials Inc.) was etched in HF:HNO_3 solution for preparation of SiC NCs. The synthesis method was reported elsewhere[49]. Briefly, SiC powder was placed in an acid digestion chamber with concentrated HF:HNO_3 solutions and etched for 2 hours at 100 °C. During the etching a thin porous layer is formed on the surface of the particles. After removing the acid and sonication of the porous SiC we obtain 1-5 nm SiC NCs and large particles residue that can be removed by centrifugation. Repeating the etching process on the microparticles, they shrink slowly and the size distribution

of the nanoparticles becomes wider. The samples were studied by photoluminescence (PL; Horiba Jobin Yvon NanoLog), atomic force microscopy (AFM; NeaSpec), and high resolution transmission electron microscopy (HRTEM; JEOL JEM-3010). The PL was measured with a 450 W Xe lamp and 3 nm bandwidth for SiC colloid solution unless noted. We applied a standard spin coating technique to separate the nanoparticles dried on a silicon substrate, in order to study them by AFM. For size distribution measurements, about 300 particles were measured with AFM on different places of the substrate. We deposited the dried SiC particles on a thin carbon layer for HRTEM study and about 300 particles were analyzed.

Acknowledgement A.G. acknowledges the funding support from the Hungarian OTKA Grants No. 101819 and 106114, and the MTA Lendület programme from the Hungarian Academy of Sciences. K.K. and Zs.Sz. acknowledge the funding support from the Hungarian OTKA Grant no. 105691.

references

(1) Rosario, G. *Properties and Applications of Silicon Carbide*; InTech 2011, ISBN 978-953-307-201-2.

(2) Palmour, J. W.; Edmond, J. A.; Kong, H. S.; Carter, C. H. 6H-Silicon Carbide Devices and Applications. *Phys. B Condens. Matter* **1993**, *185*, 461–465.

(3) Mehregany, M. SiC MEMS: Opportunities and Challenges for Applications in Harsh Environments. *Thin Solid Films* **1999**, *355-356*, 518–524.

(4) Powell, A. Growth Of Sic Substrates. *Int. J. High Speed Electron. Syst.* **2006**, *16*, 751.

(5) Koehl, W. F.; Buckley, B. B.; Heremans, F. J.; Calusine, G.; Awschalom, D. D. Room Temperature Coherent Control of Defect Spin Qubits in Silicon Carbide. *Nature* **2011**, *479*, 84–87.

(6) Falk, A. L.; Klimov, P. V.; Buckley, B. B.; Ivády, V.; Abrikosov, I. A.; Calusine, G.; Koehl, W. F.; Gali, Á.; Awschalom, D. D. Electrically and Mechanically Tunable Electron Spins in Silicon Carbide Color Centers. *Phys. Rev. Lett.* **2014**, *112*, 187601.

(7) Castelletto, S.; Johnson, B. C.; Ivády, V.; Stavrias, N.; Umeda, T.; Gali, A.; Ohshima, T. A Silicon Carbide Room-Temperature Single-Photon Source. *Nat. Mater.* **2014**, *13*, 151–156.

(8) Widmann, M.; Lee, S.-Y.; Rendler, T.; Son, N. T.; Fedder, H.; Paik, S.; Yang, L.-P.; Zhao, N.; Yang, S.; Booker, I.; et al. Coherent Control of Single Spins in Silicon Carbide at Room Temperature. *Nat. Mater.* **2015**, *14*, 164–168.

(9) David J. Christle, Abram L. Falk, Paolo Andrich, Paul V. Klimov, Jawad Ul Hassan, Nguyen T. Son, Erik Janzén, Takeshi Ohshima, D. D. A. Isolated Electron Spins in Silicon Carbide with Millisecond-Coherence Times. *Nat. Mater.* **2015**, *14*, 160–163.

(10) Morkoç, H.; Strite, S.; Gao, G. B.; Lin, M. E.; Sverdlov, B.; Burns, M. Large-Band-Gap SiC, III-V Nitride, and II-VI ZnSe-Based Semiconductor Device Technologies. *J. Appl. Phys.* **1994**, *76*, 1363.

(11) Shin, W.; Seo, W.; Takai, O.; Koumoto, K. Surface Chemistry of Porous Silicon Carbide. *J. Electron. Mater.* **1998**, *27*, 304–307.

(12) Mwania, M.; Janáky, C.; Rajeshwar, K.; Kroll, P. Fabrication of B-SiC Quantum Dots by Photo-Assisted Electrochemical Corrosion of Bulk Powders. *Electrochem. commun.* **2013**, *37*, 1–4.

(13) FAN, J.; WU, X.; CHU, P. Low-Dimensional SiC Nanostructures: Fabrication, Luminescence, and Electrical Properties. *Prog. Mater. Sci.* **2006**, *51*, 983–1031.

(14) Somogyi, B.; Gali, A. Computational Design of in Vivo Biomarkers. *J. Phys. Condens. Matter* **2014**, *26*, 143202.

(15) Barillet, S.; Jugan, M.-L.; Laye, M.; Leconte, Y.; Herlin-Boime, N.; Reynaud, C.; Carrière, M. In Vitro Evaluation of SiC Nanoparticles Impact on A549 Pulmonary Cells: Cyto-, Genotoxicity and Oxidative Stress. *Toxicol. Lett.* **2010**, *198*, 324–330.

(16) Schettini, N.; Jaroszeski, M. J.; West, L.; Saddow, S. E. *Hemocompatibility Assessment of 3C-SiC for Cardiovascular Applications in Silicon Carbide Biotechnology, 1st edition, Chapter 5,* Elsevier Inc., 2012. *pp.153-208, ISBN: 978-0-12-385906-8.*

(17) Fan, J.; Wu, X.; Zhao, P.; Chu, P. Stability of Luminescent 3C-SiC Nanocrystallites in Aqueous Solution. *Phys. Lett. A* **2006**, *360*, 336–338.

(18) Beke, D.; Szekrényes, Z.; Balogh, I.; Veres, M.; Fazakas, E.; Varga, L. K.; Kamarás, K.; Czigány, Z.; Gali, A. Characterization of Luminescent Silicon Carbide Nanocrystals

Prepared by Reactive Bonding and Subsequent Wet Chemical Etching. *Appl. Phys. Lett.* **2011**, *99*, 213108.

(19) Beke, D.; Szekrényes, Z.; Pálfi, D.; Róna, G.; Balogh, I.; Maák, P. A.; Katona, G.; Czigány, Z.; Kamarás, K.; Rózsa, B.; et al. Silicon Carbide Quantum Dots for Bioimaging. *J. Mater. Res.* **2013**, *28*, 205–209.

(20) Botsoa, J.; Lysenko, V.; Géloën, a.; Marty, O.; Bluet, J. M.; Guillot, G. Application of 3C-SiC Quantum Dots for Living Cell Imaging. *Appl. Phys. Lett.* **2008**, *92*, 173902.

(21) Mognetti, B.; Barberis, A.; Marino, S.; Di Carlo, F.; Lysenko, V.; Marty, O.; Géloën, A. Preferential Killing of Cancer Cells Using Silicon Carbide Quantum Dots. *J. Nanosci. Nanotechnol.* **2010**, *10*, 7971–7975.

(22) Matsumoto, T.; Takahashi, J.; Tamaki, T.; Futagi, T.; Mimura, H.; Kanemitsu, Y. Blue-Green Luminescence from Porous Silicon Carbide. *Appl. Phys. Lett.* **1994**, *64*, 226.

(23) Rittenhouse, T. L. Surface-State Origin for the Blueshifted Emission in Anodically Etched Porous Silicon Carbide. *J. Appl. Phys.* **2004**, *95*, 490.

(24) Szekrényes, Z.; Somogyi, B.; Beke, D.; Károlyházy, G.; Balogh, I.; Kamarás, K.; Gali, A. Chemical Transformation of Carboxyl Groups on the Surface of Silicon Carbide Quantum Dots. *J. Phys. Chem. C* **2014**, *118*, 19995–20001.

(25) Dai, D.; Guo, X.; Fan, J. Identification of Luminescent Surface Defect in SiC Quantum Dots. *Appl. Phys. Lett.* **2015**, *106*, 053115.

(26) Vörös, M.; Deák, P.; Frauenheim, T.; Gali, A. The Absorption of Oxygenated Silicon Carbide Nanoparticles. *J. Chem. Phys.* **2010**, *133*, 064705.

(27) Vörös, M.; Deák, P.; Frauenheim, T. Time-Dependent Density Functional Calculations on Hydrogenated Silicon Carbide Nanocrystals. *Mater. Sci. Forum* **2011**, *679-680*, 516-519.

(28) Vörös, M.; Deák, P.; Frauenheim, T.; Gali, A. The Absorption Spectrum of Hydrogenated Silicon Carbide Nanocrystals from Ab Initio Calculations. *Appl. Phys. Lett.* **2010**, *96*, 051909.

(29) Wu, X.; Fan, J.; Qiu, T.; Yang, X.; Siu, G.; Chu, P. Experimental Evidence for the Quantum Confinement Effect in 3C-SiC Nanocrystallites. *Phys. Rev. Lett.* **2005**, *94*, 026102.

(30) Bhunia, S. K.; Saha, A.; Maity, A. R.; Ray, S. C.; Jana, N. R. Carbon Nanoparticle-Based Fluorescent Bioimaging Probes. *Sci. Rep.* **2013**, *3*, 1473.

(31) Chandra, S.; Pathan, S. H.; Mitra, S.; Modha, B. H.; Goswami, A.; Pramanik, P. Tuning of Photoluminescence on Different Surface Functionalized Carbon Quantum Dots. *RSC Adv.* **2012**, *2*, 3602-3606.

(32) Dong, Y.; Shao, J.; Chen, C.; Li, H.; Wang, R.; Chi, Y.; Lin, X.; Chen, G. Blue Luminescent Graphene Quantum Dots and Graphene Oxide Prepared by Tuning the Carbonization Degree of Citric Acid. *Carbon* **2012**, *50*, 4738–4743.

(33) Zhu, S.; Song, Y.; Zhao, X.; Shao, J.; Zhang, J.; Yang, B. The Photoluminescence Mechanism in Carbon Dots (graphene Quantum Dots, Carbon Nanodots and Polymer Dots): Current State and Future Perspective. *Nano Res.* **2015,** *8*, 355-381..

(34) Guo, X.; Dai, D.; Fan, B.; Fan, J. Experimental Evidence of A → B Phase Transformation in SiC Quantum Dots and Their Size-Dependent Luminescence. *Appl. Phys. Lett.* **2014**, *105*, 193110.

(35) Choi, H. S.; Liu, W.; Misra, P.; Tanaka, E.; Zimmer, J. P.; Itty Ipe, B.; Bawendi, M. G.; Frangioni, J. V. Renal Clearance of Quantum Dots. *Nat. Biotechnol.* **2007**, *25*, 1165–1170.

(36) Zhang, X. D.; Yang, J.; Song, S. S.; Long, W.; Chen, J.; Shen, X.; Wang, H.; Sun, Y. M.; Liu, P. X.; Fan, S. Passing through the Renal Clearance Barrier: Toward Ultrasmall Sizes with Stable Ligands for Potential Clinical Applications. *Int. J. Nanomedicine* **2014**, *9*, 2069–2072.

(37) Wei, G.; Qin, W.; Wang, G.; Sun, J.; Lin, J.; Kim, R.; Zhang, D.; Zheng, K. The Synthesis and Ultraviolet Photoluminescence of 6H–SiC Nanowires by Microwave Method. *J. Phys. D. Appl. Phys.* **2008**, *41*, 235102.

(38) Emelchenko, G.; Zhokhov, A.; Tartakovskii, I. I.; Maksimov, A.; Steinman, E. On Peculiarities of Defect Formation in 6H-SiC Bulk Single Crystals Grown by PVT Method. *Mater. Sci. Forum* **2013**, *740-742*, 43–47.

(39) Cambaz, G. Z.; Yushin, G. N.; Gogotsi, Y.; Lutsenko, V. G. Anisotropic Etching of SiC Whiskers. *Nano Lett.* **2006**, *6*, 548–551.

(40) Zhu, J.; Hu, S.; Xia, W.; Li, T.; Fan, L.; Chen, H. Photoluminescence of ~2nm 3C–SiC Quantum Dots Fabricated from Polycrystalline 6H–SiC Target by Pulsed Laser Ablation. *Mater. Lett.* **2014**, *132*, 210–213.

(41) Vlaskina, S. I.; Mishinova, G. N.; Vlaskin, V. I.; Rodionov, V. E.; Svechnikov, G. S. 3C-6H Transformation in Heated Cubic Silicon Carbide 3C-SiC. *Semicond. Physics, Quantum Electron. Optoelectron.* **2011**, *14*, 432–436.

(42) A.A. Gippius, R. Helbig, J. P. F. S. *SiC, Natural and Synthetic Diamond and Related Materials*, 1st ed.; Elsevier B.V. North-holland: Amsterdam, 1991, ISBN: 9780444596772

(43) Kagan, C.; Murray, C.; Bawendi, M. Long-Range Resonance Transfer of Electronic Excitations in Close-Packed CdSe Quantum-Dot Solids. *Phys. Rev. B* **1996**, *54*, 8633–8643.

(44) Mićić, O. I.; Ahrenkiel, S. P.; Nozik, A. J. Synthesis of Extremely Small InP Quantum Dots and Electronic Coupling in Their Disordered Solid Films. *Appl. Phys. Lett.* **2001**, *78*, 4022.

(45) Sarkar, S. K.; Hodes, G. Charge Overlap Interaction in Quantum Dot Films: Time Dependence and Suppression by Cyanide Adsorption. *J. Phys. Chem. B* **2005**, *109*, 7214–7219.

(46) Yang, S.; Kiraly, B.; Wang, W. Y.; Shang, S.; Cao, B.; Zeng, H.; Zhao, Y.; Li, W.; Liu, Z.-K.; Cai, W.; et al. Fabrication and Characterization of Beaded SiC Quantum Rings with Anomalous Red Spectral Shift. *Adv. Mater.* **2012**, *24*, 5598–5603.

(47) Somogyi, B.; Zólyomi, V.; Gali, A. Near-Infrared Luminescent Cubic Silicon Carbide Nanocrystals for in Vivo Biomarker Applications: An Ab Initio Study. *Nanoscale* **2012**, *4*, 7720–7726.

(48) Krueger, A.; Astakhov, G. V; Muzha, A.; Fuchs, F.; Tarakina, N. V; Simin, D.; Trupke, M.; Soltamov, V. A. Room-Temperature near-Infrared Silicon Carbide Nanocrystalline Emitters Based on Optically Aligned Spin Defects. *Appl. Phys. Lett.* **2014**, *105, 243112*.

(49) Beke, D.; Szekrényes, Z.; Balogh, I.; Czigány, Z.; Kamarás, K.; Gali, A. Preparation of Small Silicon Carbide Quantum Dots by Wet Chemical Etching. *J. Mater. Res.* **2013**, *28*, 44–49.